

# DFT Study of Structure and Binding Energies of Fe–Corannulene Complex

Anil K. Kandalam,\* B. K. Rao,† and P. Jena

Physics Department, Virginia Commonwealth University, Richmond, Virginia 23284

Received: May 19, 2005; In Final Form: August 12, 2005

Density functional theory (DFT) based theoretical calculations are performed to identify the ground-state geometries, the spin multiplicities, and the relevant energetics of neutral and positively charged Fe–corannulene complexes. Our calculations show that the on-top site of the six-membered ring ( $\eta^6$ ) of corannulene molecule is the most preferred binding site for both Fe atom and Fe<sup>+</sup> ion. The electrostatic potential (ESP) surface picture is employed to explain the preference of the  $\eta^6$ - over the  $\eta^5$ -binding site (on-top site of central pentagon) of corannulene. Though in both neutral and cationic species the  $\eta^6$ -site is the most preferred binding site, the ground-state geometries of these complexes are different. The Fe<sup>+</sup> cation prefers to bind to the convex face of the corannulene, whereas the neutral Fe atom prefers slightly the concave to the convex face. The ionization-induced structural changes are reflected in the large energy difference between the vertical and adiabatic ionization potential values. We also show that the dissociation of Fe<sup>+</sup>–corannulene complex to corannulene + Fe<sup>+</sup> is just as likely as that to Fe + (corannulene)<sup>+</sup>.

## I. Introduction

Study of the interactions of metal atoms and ions with polycyclic aromatic hydrocarbons (PAHs) is of central interest to organometallic chemistry as they play an important role in environmental and interstellar problems as well as in cluster-assembled materials, drug–receptor interactions, and substrate binding and biological processes. A fundamental understanding of these intermolecular interactions is possible through the gas-phase studies of organometallic complexes where the effect of the solvent does not complicate the problem. Most of these studies, however, have been limited to metal atoms and ions deposited on flat surfaces starting from organic molecules such as benzene and coronene to graphite.

The discovery of C<sub>60</sub> fullerene has given rise to a great deal of interest in the study of metal atom and ion interactions with curved surfaces. Corannulene (C<sub>20</sub>H<sub>10</sub>) is among the simplest example of a curved carbon  $\pi$ -system, where the bowl-shaped C<sub>20</sub> can be considered a fragment of the C<sub>60</sub> fullerene. Because of the intrinsic curvature of this molecule, it possesses two curved surfaces—convex and concave. Unlike the case of metal atom/ion interactions with a planar  $\pi$ -conjugated structure such as coronene, where both faces are equivalent, the interaction with curved surfaces is complicated because there are not only a number of sites ( $\eta^2$ ,  $\eta^4$ ,  $\eta^5$ , and  $\eta^6$ ) where metal atoms can attach, but also one has to investigate these sites on either side of the surface. For example, recent work by Dunbar<sup>1</sup> shows that Ti<sup>+</sup> and Ni<sup>+</sup> prefer to bind over the six-membered ring on the convex face, whereas Cr<sup>+</sup> adsorbs on the five-membered ring, similar to that for alkali metal cations. In contrast, Cu<sup>+</sup> prefers to bind at the edge site rather than the ring centers. These results reveal that each transition metal atom binds differently on corannulene and the differences could be due to the chemical bonding with that of the corannulene surface. Although recent theoretical studies<sup>1,2</sup> have concentrated on the interaction of metal cations (Li<sup>+</sup>, Na<sup>+</sup>, K<sup>+</sup>, Ti<sup>+</sup>, Cr<sup>+</sup>, Ni<sup>+</sup>, Cu<sup>+</sup>) with

corannulene, corresponding neutral atom interactions are not available. In a very recent gas-phase experimental study,<sup>3</sup> Duncan and co-workers reported the synthesis of positively charged metal–corannulene molecules and mixed ligand complexes such as Fe<sup>+</sup>(cyclopentadienyl)(corannulene) and Fe<sup>+</sup>(cyclopentadienyl)(benzene). The mixed ligand complexes were produced by covaporization of Fe<sup>+</sup>(cyclopentadienyl)(benzene) and corannulene. The reactivity of C<sub>60</sub>Fe<sup>+</sup> and C<sub>20</sub>H<sub>10</sub>Fe<sup>+</sup> complexes was reported in a recent gas-phase experimental study.<sup>4</sup> However, from these experimental studies accurate information regarding the equilibrium geometry, ground-state spin multiplicities, and electronic structure of Fe<sup>+</sup>–corannulene complex cannot be obtained.

Currently, theoretical calculations are the only way to investigate the geometry of these complexes and to determine the most preferred adsorption site of neutral and cationic Fe. In addition, theory can also shed light on the electronic structure and bonding of metal atom/ion on corannulene substrate. The objective of the present study is 2-fold: First we study the interaction of Fe<sup>+</sup> with corannulene and compare that with the previously published results of other metal cations; Second, we investigate how the interactions of cations differ from those of neutral metal atoms, which so far have not been investigated. Using density functional theory, we have studied the equilibrium geometries, the preferred bonding sites of the Fe and Fe<sup>+</sup> ion, the dissociation energies, and the ionization potentials. The results are compared with available experimental data and previous theoretical calculations. In section II, we briefly describe our computational procedure. The results are presented and discussed in section III, and finally we summarize our results in Section IV.

## II. Computational Procedure

Calculations using density functional theory (DFT) with generalized gradient approximation (GGA) for exchange and correlation potential are performed to identify the ground-state geometries of neutral and positively charged (Fe–corannulene) complexes. We have used the gradient corrected exchange

\* Corresponding author. E-mail address: akkandalam@vcu.edu.

† Deceased.

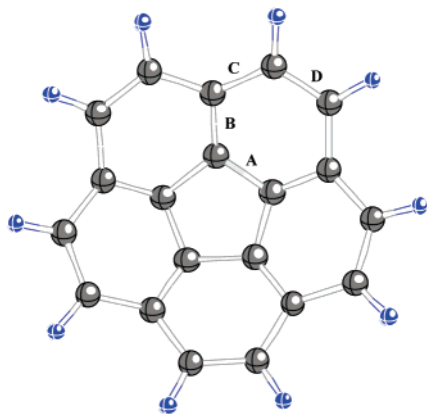


**Figure 1.** Corannulene molecule, with the four different types of C–C bonds identified.

functional due to Becke,<sup>5</sup> in conjunction with the gradient corrected Perdew–Wang<sup>6</sup> correlation functional (BPW91). Another form of GGA functional that is commonly used for studying organic systems is referred to as B3LYP. However, previous works<sup>7,8</sup> have shown that, while the B3LYP functional provides accurate energies for organic systems, it is not as good for organometallic systems. For example, Stockigt<sup>7</sup> has shown that B3LYP-based results generally gave lower binding energies than those obtained using BPW91 for the Al–benzene complex. In another DFT (B3LYP) study<sup>8</sup> of the binding energies of cationic transition metal–organic systems, it was reported that the binding energies differed from the experimental values by several kilocalories per mole. We have repeated some of our calculations using the B3LYP functional for the Fe–corannulene complex, and our results are consistent with the above conclusion. Moreover, the reliability and accuracy of the BPW91 functional has also been confirmed in our previous calculations on  $V_n(\text{Bz})_m$ <sup>9</sup> and  $Ni_n(\text{Bz})_m$ <sup>10</sup> complexes. In what follows, we will report only results based on the BPW91 functional. We have employed an all-electron 6-311G\*\* basis set in this work. The accuracy of this basis set was tested by first calculating the ionization potential (IP) of corannulene molecule. Our calculated vertical IP of 7.88 eV for the corannulene molecule agrees well with the experimental IP value<sup>11</sup> of  $7.83 \pm 0.02$  eV. To test the adequacy and completeness of this basis set further, we have performed optimization calculations on the two lowest energy isomers of Fe–corannulene complex using a larger basis set containing diffuse functions, namely 6-311+G\* for Fe atom. A maximum difference of 0.04 Å is seen between the various equilibrium distances obtained from the two basis sets. The relative energy ordering between the two lowest energy isomers remained the same, with the energy difference changing from 0.13 to 0.08 eV in the neutral complex, whereas in the cationic complex the energy difference changed from 0.32 to 0.28 eV. Overall, this proves that the effect of including diffuse functions on the metal atom is small and the 6-311G\*\* basis set is expected to give satisfactory results for this system.

The identification of the ground-state geometry of Fe–corannulene is a complex problem as there are a wide variety of binding sites where an Fe atom can attach to the corannulene molecule. Hence, to identify the ground-state geometry (i.e., the most preferred Fe binding site on corannulene), different starting configurations were considered in the geometry optimization procedure. These geometries were completely optimized without any symmetry constraints for all the possible spin multiplicities. In the geometry optimization procedure, the convergence criteria for gradient force and energy are set to  $10^{-4}$  hartree/Å and  $10^{-9}$  hartree, respectively. The stability of

**TABLE 1: Various C–C Bond Lengths (Å) of Neutral Corannulene Molecule<sup>a</sup>**

C–C bonds	theory		experiment	
	this work	(B3LYP/6-31G*) <sup>a</sup>	gas phase <sup>a</sup>	crystal <sup>b</sup>
A	1.420	1.417	1.410	1.419
B	1.392	1.385	1.408	1.394
C	1.449	1.448	1.441	1.443
D	1.394	1.390	1.374	

<sup>a</sup> Reference 13. <sup>b</sup> Reference 14.

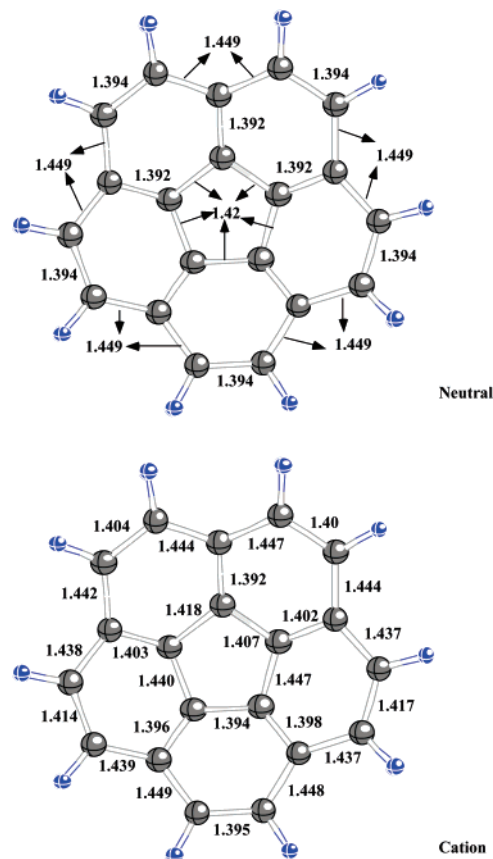


**Figure 2.** Optimized geometries of neutral and cationic corannulene. All bond lengths are in angstroms.

the ground-state geometry was confirmed by computing vibrational frequencies. All calculations in this work were performed using the Gaussian 98<sup>12</sup> program suite.

### III. Results and Discussion

**A. Geometries.** In this section, we first discuss the geometry of corannulene molecule followed by the ground-state geometries of neutral and positively charged (Fe–corannulene) complexes.

*Corannulene Molecule.* Corannulene is a bowl-shaped molecule containing a five-membered ring (pentagon) in its center and five six-membered rings (hexagons), where each of these hexagons is fused to each other and to the sides of the central pentagon. The equilibrium geometry of corannulene molecule is given in Figure 1. The neutral corannulene molecule has  $C_{5v}$  symmetry. There are four different types of C–C bonds in the neutral corannulene molecule. These are labeled “A”, “B”, “C”, and “D”, starting with the inner C–C bond, which is common to both the pentagonal and hexagonal rings, and proceeding in the clockwise direction along the hexagonal ring (see Figure 1). The optimized structural parameters of neutral corannulene, along with the corresponding experimental bond lengths, are

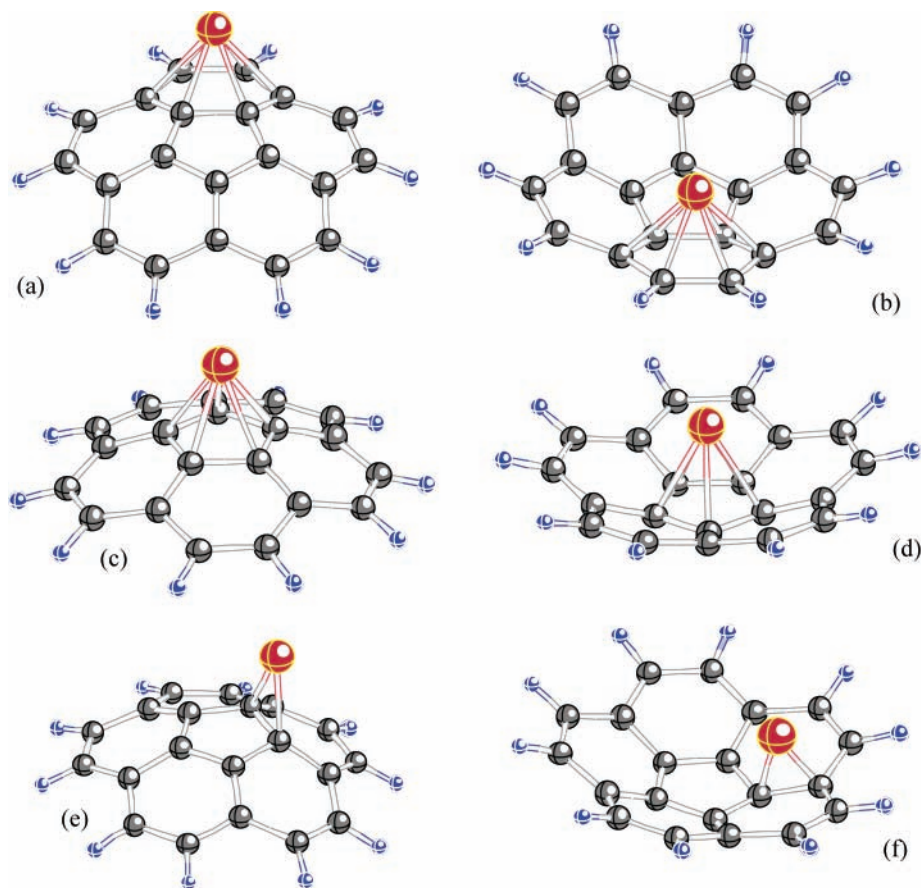


**Figure 3.** Different starting structures considered for the geometry optimization of neutral and positively charged (Fe–corannulene) complexes.

given in Table 1. Our calculated bond lengths, with the exception of bond D, are in good agreement with the previous theoretical and corresponding experimental gas-phase data<sup>13</sup> as well as with the crystallographic data.<sup>14</sup>

The optimized geometry of positively charged corannulene, along with its structural parameters, is given in Figure 2. The equilibrium geometry of neutral corannulene is also included for comparison. The ground-state spin multiplicity of the corannulene ion is a doublet ( $2S + 1 = 2$ ). As we can see from Figure 2, the removal of an electron from corannulene has resulted in small but significant changes in the C–C bond distances. The cationic corannulene has  $C_1$  symmetry because of charge-induced Jahn–Teller distortion. The maximum variation in C–C bond lengths from the corresponding bond lengths in the neutral molecule is seen in bond A, namely in the bonds making up the central pentagon. Most of the C–C bonds in the pentagon, with the exception of one of them, have relaxed, but not in equal amounts with a maximum relaxation of 0.027 Å. Similarly, bond B and bond D have seen a maximum relaxation of 0.011 Å. However, the most important observation here is that the corannulene ion is asymmetric and the number of different types of C–C bonds is no longer four.

The vertical and adiabatic IPs of corannulene are calculated to be 7.88 and 7.55 eV, respectively. Our calculated results are in good agreement with the previously reported<sup>11</sup> B3LYP/6-311G\*\* based values of 7.71 (vertical IP) and 7.58 eV (adiabatic IP) and the experimental value<sup>11</sup> of  $7.83 \pm 0.02$  eV. The structural differences, especially the symmetry breaking and charge-induced distortions, between the positively charged corannulene ion and its neutral species are reflected in the large energy difference ( $\sim 0.33$  eV) between the vertical and adiabatic values of IP.

*Fe–Corannulene Complex.* Corannulene molecule, due to its curved surface, unlike benzene and coronene, offers Fe atom binding sites on both the concave (inside) and convex (outside) faces of the bowl. Also, on a given face/site of the bowl, the metal atom can occupy either the on-top site above the five-membered ring ( $\eta^5$ -site) or the on-top site above one of the six-membered rings ( $\eta^6$ -site). The metal atom can also occupy any of the bridge sites ( $\eta^2$ -site) above various C–C bonds such as bond A or bond B. We have taken into account all these possibilities by considering six different structural configurations for the geometry optimization. In Figure 3, we present all these different starting geometries. Some of these structures after geometry optimization resulted in the same final structure, while some others led to different structures. Figure 4 shows the ground-state geometry along with its equilibrium structural parameters of neutral Fe–corannulene complex and its next higher energy isomer.

Our calculations revealed the geometry in which the Fe atom located on the  $\eta^6$ -site on the concave side (inside) of the bowl as the most favored structure (Figure 4a). The corresponding outside- $\eta^6$ -structure (Figure 4b) is energetically very close with an energy difference of 0.136 eV. Thus, the concave- and convex- $\eta^6$ -binding sites compete in stabilizing the Fe–corannulene complex. At the current level of our computational accuracy, one cannot distinctly identify if the ground-state geometry of neutral Fe–Corannulene complex is the outside- $\eta^6$ - or inside- $\eta^6$ -structure. It should be noted here that in both the inside- and outside- $\eta^6$ -site geometries the Fe atom is not exactly centered on top of the hexagonal ring, which is similar to the recently reported<sup>15</sup> ground-state geometry of Fe–coronene complex. The bond lengths of the Fe–C vary from 1.98 to 2.11 Å. The binding of Fe atom to the  $\eta^6$ -site of the corannulene

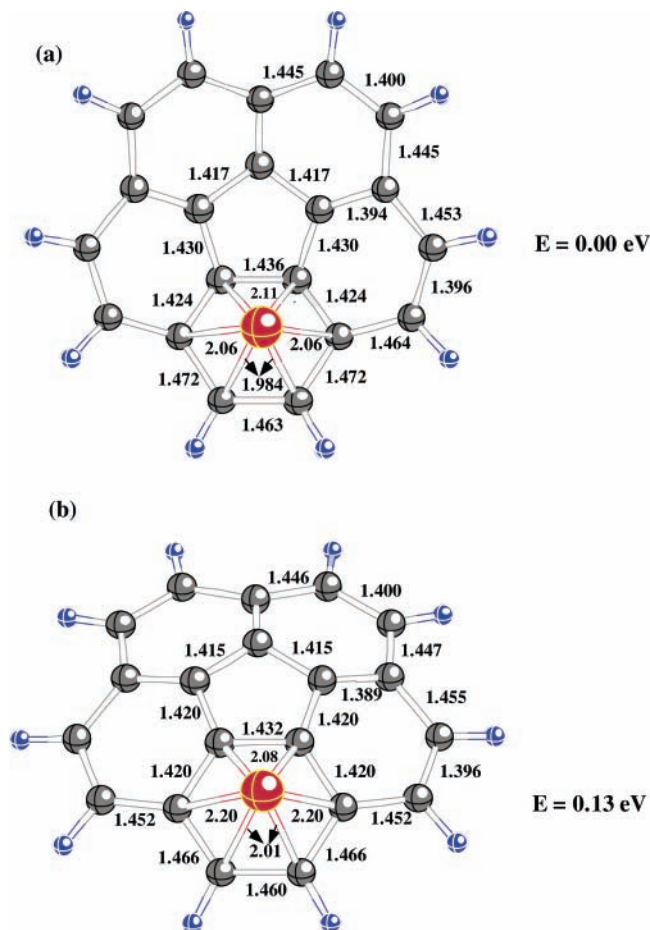


**Figure 4.** Lowest energy and the next higher energy isomers of neutral (Fe–corannulene) complex. The relative energies, calculated with respect to the ground-state geometry, are also shown.

**TABLE 2: Relative Energies (in eV) of Various Binding Sites on Corannulene**

system	convex			concave		
	$\eta^6$	$\eta^5$	$\eta^2$	$\eta^6$	$\eta^5$	$\eta^2$
Fe–corannulene	0.136	–	0.825	0.000	–	–
(Fe–corannulene) <sup>+</sup>	0.000	0.451	–	0.325	0.870	–

has resulted in small stretching of C–C bonds in the hexagonal ring of corannulene. The maximum effect is seen on bond D with a stretching of 0.069 Å in inside- $\eta^6$ -site and 0.066 Å in outside- $\eta^6$ -site geometries, while the other C–C bonds in the hexagon have relaxed by a maximum of 0.03 Å compared to the corresponding bond lengths in a free corannulene molecule.

In the other structural isomers, the starting geometries with Fe on the concave side of the  $\eta^5$  complex (Figure 3d) and that on top of the bridge site above bond B (Figure 3f) yielded the same geometry, namely Fe bound on the concave side of the  $\eta^6$  geometries. The optimization of the structure when the Fe atom was initially placed on the outside of the  $\eta^5$  configuration (Figure 3c) yielded a structure where the Fe atom lies on top of the C–C bridge site over bond A. The relative energies corresponding to various binding sites on corannulene are collected in Table 2.

We would like to point out here that, although in two of our starting geometries the Fe atom was placed at the  $\eta^5$ -sites, after geometry relaxation the Fe atom either completely migrated toward the neighboring  $\eta^6$ -site or at least moved halfway through, reaching the  $\eta^2$ -site. Therefore, in neutral Fe–coran-

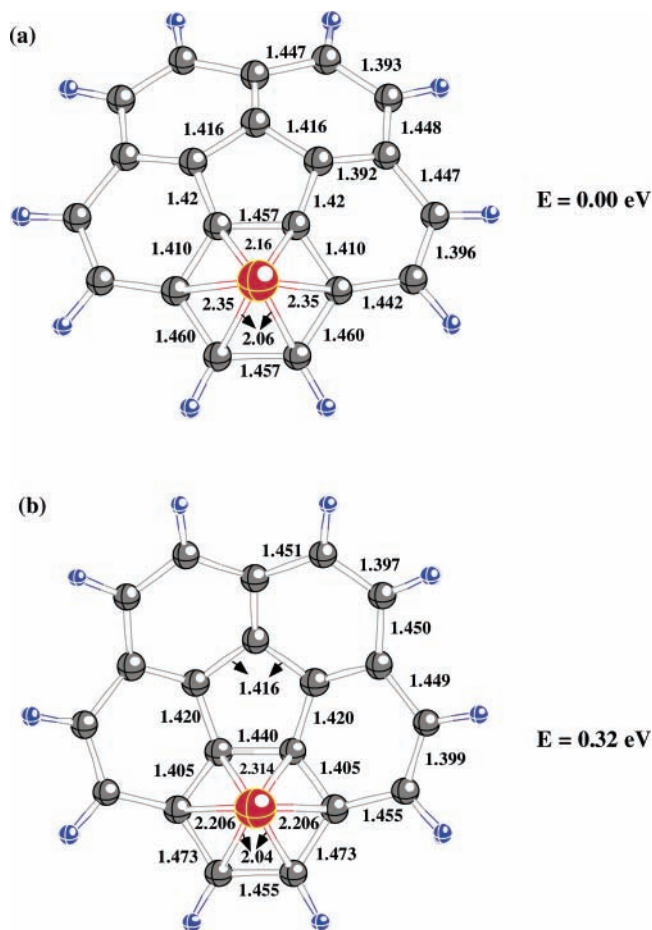


**Figure 5.** Lowest energy and next higher energy isomers of positively charged (Fe–corannulene)<sup>+</sup> complex. The relative energies, calculated with respect to the ground-state geometries are also shown.

nulene complex, the  $\eta^5$ -binding sites do not correspond to a local minimum.

The spin multiplicities of the lowest energy and next higher energy configurations are both found to be triplet ( $2S + 1 = 3$ ). It should be noted here that the ground-state spin multiplicities for Fe–benzene<sup>16</sup> and Fe–coronene<sup>15</sup> complexes were also reported to be triplet. Thus, the change in the magnetic moment of Fe is because of its binding with corannulene, which is similar to its binding with benzene and coronene, where the magnetic moment of Fe is reduced from its atomic value of  $4\mu_B$  to  $2\mu_B$ . It will be interesting to see if a similar trend exists when a second Fe atom is added to the Fe–corannulene complex. There are no experimental results available to verify our prediction on the magnetic moment of Fe–corannulene complex. In addition, the spin multiplicities of other transition metal atoms bonded to corannulene are also not known for comparison.

*(Fe–Corannulene)<sup>+</sup> Complex.* For (Fe–corannulene)<sup>+</sup> cation, the same six starting geometries as in the neutral complex are considered for geometry optimization (see Figure 3). Figure 5 shows the ground-state geometry and the next higher energy isomer, along with the equilibrium structural parameters of the cation.

The structural configuration corresponding to the  $\eta^6$ -binding site, with Fe located on the convex (outside) face of the corannulene (Figure 5a) molecule, is the most favored structure of the (Fe–corannulene)<sup>+</sup> cation. The inside- $\eta^6$ -binding site, the most favored binding site in neutral Fe–corannulene complex, is higher in energy ( $\sim 0.325$  eV) in the case of cation (Figure 5b). Hence, the electron detachment has resulted in

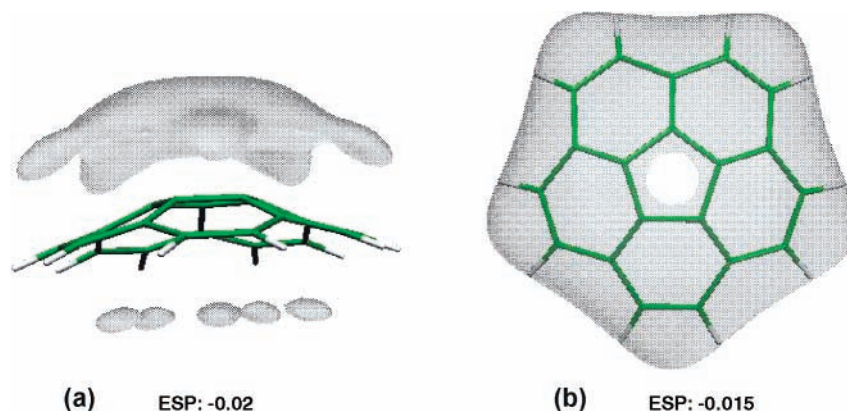


**Figure 6.** Electrostatic potential isosurface of corannulene molecule. Two orientations are shown here.

stabilizing the outside- $\eta^6$ -site more than the inside- $\eta^6$ -site by 0.46 eV. It is important to note here that the energy required for the inversion of the corannulene molecule at room temperature was reported<sup>17</sup> to be about 10 kcal mol<sup>-1</sup> ( $\sim 0.43$  eV). In our calculations the energy difference between the structures with convex (outside) and concave (inside)  $\eta^6$ -binding sites is 0.325 eV. This energy difference is significant at this current level of theory and suggests that the inside- $\eta^6$ -site is the preferred binding site. However, under kinetic control conditions, either of these structures is expected to form and switching from one structure to the other by a simple inversion of corannulene is not expected to occur. In a previously reported investigation<sup>4</sup> on the gas-phase reactivity of Fe–corannulene cation, it was predicted that the corannulene binds to Fe cation in either a  $\eta^4$  or a  $\eta^6$  fashion. However, these experimental results also could not determine if the Fe ion is on the convex or concave face of corannulene. On the basis of the inversion energy of the corannulene molecule, the authors interpreted that the endohedral and exohedral binding sites are interchangeable.

From Table 2, it is immediately clear that, in cationic (Fe–corannulene)<sup>+</sup> complex, the geometries corresponding to  $\eta^5$ -binding sites are found to be local minima, with the convex side being more favorable than the concave side. In addition, contrary to what was seen in neutral Fe–corannulene, the  $\eta^2$ -binding sites are not favorable for Fe<sup>+</sup> ion. For example, when the Fe is placed on top of the C–C bridge site over bond A, it moved to the on-top site of the central pentagon ( $\eta^5$ -site).

It is noteworthy here that the energy difference between the convex- and concave- $\eta^5$ -sites is larger when compared to the energy difference between the corresponding convex-/concave- $\eta^6$ -sites (0.420 eV vs 0.325 eV). This observation is consistent with the previously reported results<sup>1</sup> on Ti<sup>+</sup>–, Cr<sup>+</sup>–, and Ni<sup>+</sup>–corannulene complexes. In this work, it was reported that the average energy difference between the concave- and convex- $\eta^5$ -binding sites is almost 0.47 eV, whereas it is 0.17 eV for concave-/convex- $\eta^6$ -binding sites.

In summary, the relative stabilities of various binding sites in cationic (Fe–corannulene)<sup>+</sup> can be given as follows: concave- $\eta^5$ -site < convex- $\eta^5$ -site < concave- $\eta^6$ -site < convex- $\eta^6$ -site. In the previous theoretical study,<sup>1</sup> it was reported that Ti<sup>+</sup>, Cr<sup>+</sup>, and Ni<sup>+</sup> favored the  $\eta^6$ -sites over the  $\eta^5$ -sites. It was also reported that the outside- $\eta^6$ -site is more favorable than the corresponding inside one, but only by a small amount and, among the  $\eta^5$ -sites, the convex side is preferred. Our calculations on the binding of Fe ion to various corannulene binding sites have also resulted in a similar conclusion.

To understand why the convex- $\eta^6$ -site is the most preferred site for adsorption of Fe atom or ion on the corannulene, we have plotted the electrostatic potential (ESP) surface of the

corannulene molecule as shown in Figure 6. The front view of the electrostatic potential surface at the isosurface value of  $-0.002$  is shown Figure 6a. It is clear from the figure that Fe<sup>+</sup> being an electrophile in nature would prefer to reside on the convex surface than on the concave. Further verification of the preferential binding of Fe on the peripheral hexagon over the center pentagon is illustrated from the top view of the ESP surface as shown in Figure 6b. Though the electrostatic effects explain the preference of certain binding sites over others, it should be noted here that there are also significant electronic effects playing a role in these complexes. Our idea here is to give a simple qualitative picture from the electrostatic viewpoint.

**B. Energetics.** In this section, the dissociation energies, ionization potential (IP), and electron affinity of the Fe–corannulene complex are presented and discussed.

We first start our discussion with the IP calculations. The IPs are calculated following the definition  $IP = \text{energy}_{\text{cation}} - \text{energy}_{\text{neutral}}$ . The vertical IP value corresponds to the energy difference between the cation and the neutral complex with both of them at the neutral ground-state geometry. In the adiabatic IP calculation, both the cation and neutral systems are in their respective ground-state geometries. The calculated vertical IP of Fe–corannulene complex is 5.89 eV, whereas the adiabatic IP is 5.37 eV. No experimental or theoretical data are available to compare with our calculated IP values of this system. There is a significant energy difference of 0.52 eV between the vertical and adiabatic IP values. This is attributed to the fact that the ground-state geometries of neutral and cationic complexes are not similar, with the inside- $\eta^6$ -structure in neutral and the outside- $\eta^6$ -structure in cation being the ground-state geometries.

We now turn to the dissociation energies of the neutral and positively charged Fe–corannulene complexes. The dissociation energies of the neutral complex into fragments of Fe atom and corannulene molecules are calculated as

$$D_e[\text{Fe–corannulene}] = - [E(\text{Fe–corannulene}) - E(\text{Fe}) - E(\text{corannulene})]$$

In the case of cationic (Fe–corannulene)<sup>+</sup> complex, there are two different pathways available for dissociation/fragmentation into smaller products. The dissociation/fragmentation energies of neutral and cationic complexes for different pathways are collected in Table 3. It should be noted here that since the calculated ionization potentials of Fe and corannulene molecule are very close, the fragmentation of (Fe–corannulene)<sup>+</sup> is quite interesting. Between the two available dissociation paths, dissociation into Fe<sup>+</sup> ion and neutral corannulene is energetically more favorable than dissociation into neutral Fe atom and corannulene<sup>+</sup> by 0.10 eV. Since this energy difference is very

**TABLE 3: Dissociation Energies (eV) of Neutral and Cationic (Fe–Corannulene) Complexes along Various Dissociation Pathways**

system	dissociation path	dissociation energy (eV)
Fe(C <sub>20</sub> H <sub>10</sub> )	Fe–(C <sub>20</sub> H <sub>10</sub> )	1.25
[Fe(C <sub>20</sub> H <sub>10</sub> )] <sup>+</sup>	Fe <sup>+</sup> –(C <sub>20</sub> H <sub>10</sub> )	3.28
	Fe–(C <sub>20</sub> H <sub>10</sub> ) <sup>+</sup>	3.38

small and is within the accuracy of our calculations, both dissociation paths are possible. As mentioned above, the near equality in the ionization potential values of Fe and corannulene has resulted in two different but equally probable dissociation paths. We note from Table 3 that the binding of Fe<sup>+</sup> ion to corannulene is much stronger than the binding of corresponding Fe atom to corannulene, as expected.

We are not aware of any experimental data or theoretical study about the dissociation energy of (Fe–corannulene)<sup>+</sup> complex. However, in a previous theoretical work,<sup>1</sup> the binding energies of Ti<sup>+</sup>, Cr<sup>+</sup>, and Ni<sup>+</sup> ions to the outside- $\eta^6$ -site of corannulene were reported as follows: for Cr<sup>+</sup>, 2.04 eV; for Ni<sup>+</sup>, 3.30 eV; for Ti<sup>+</sup>, 2.83 eV. In this study the MPW1PW91 functional form with 6-311+G\* basis for the metal ion and 6-311G\*\* basis for corannulene were employed. Our calculated binding energy of Fe<sup>+</sup> ion to corannulene (3.28 eV) is qualitatively the same as the binding energies of the other reported transition metal ions to the  $\eta^6$ -site of the corannulene molecule, even though the calculations have used different exchange functionals. Though there are no direct experimental dissociation energy values available for these complexes, in the recently reported experimental study<sup>3</sup> on mixed ligand organometallic complexes it was noted that the dissociation energy of Fe<sup>+</sup>–corannulene lies between that of the Fe<sup>+</sup>–benzene (C<sub>6</sub>H<sub>6</sub>) and Fe<sup>+</sup>–cyclopentadienyl (C<sub>5</sub>H<sub>5</sub>) complexes. Since the experimental dissociation energies of Fe<sup>+</sup>–C<sub>6</sub>H<sub>6</sub> and Fe<sup>+</sup>–C<sub>5</sub>H<sub>5</sub> are, respectively, 2.15<sup>18</sup> and 3.91 eV,<sup>19</sup> it is certainly gratifying to note that our calculated dissociation energy of Fe<sup>+</sup>–corannulene complex is in agreement with the reported experimental observation.

#### IV. Summary

The equilibrium geometries and ground-state spin multiplicities of neutral and positively charged corannulene and (Fe–corannulene) complexes are obtained from ab initio calculations. In the neutral Fe–corannulene complex, the on-top site of a six-membered ring ( $\eta^6$ -site) is the most favored binding site of the Fe atom. However, in neutral complex, the exact ground-state structure could not be identified because of small energy differences between convex- $\eta^6$ - and concave- $\eta^6$ -binding sites. The on-top site of the central pentagon ( $\eta^5$ -site) could not be formed in neutral Fe–corannulene. In cationic (Fe–corannulene)<sup>+</sup>, the Fe<sup>+</sup> ion, like other transition metal ions, also favored

the  $\eta^6$ -binding site. However, in the cation, the preference for convex- $\eta^6$ -binding site over concave- $\eta^6$ -binding site is clearer than in the case of the neutral complex. In positively charged (Fe–corannulene)<sup>+</sup> ion, though binding of the Fe<sup>+</sup> ion to  $\eta^5$ -site was achieved, it is energetically not a favorable position. Both the neutral and cationic complexes are found to be stable against dissociation/fragmentation into smaller complexes. The dissociation energy calculations also revealed a stronger Fe<sup>+</sup>–corannulene binding than the binding of Fe atom and corannulene.

**Acknowledgment.** The authors thank Prof. M. A. Duncan and Dr. C. Majumder for helpful discussions. B.K.R. and P.J. also acknowledge partial support from the U.S. Department of Energy (DEFG01-96ER45579).

#### References and Notes

- (1) Dunbar, R. C. *J. Phys. Chem. A* **2002**, *106*, 9809.
- (2) Frash, M. V.; Hopkinson, A. C.; Bohme, D. K. *J. Am. Chem. Soc.* **2001**, *123*, 6687.
- (3) Ayers, T. M.; Westlake, B. C.; Preda, D. V.; Scott, L. T.; Duncan, M. A. *Organometallics* **2005**, *24*, 4573.
- (4) Caraiman, D.; Koyanagi, G.; Scott, L. T.; Preda, D. V.; Bohme, D. K. *J. Am. Chem. Soc.* **2001**, *123*, 8573.
- (5) Becke, A. D. *Phys. Rev. A* **1988**, *38*, 3098.
- (6) Perdew, J. P.; Wang, Y. *Phys. Rev. B* **1992**, *45*, 13244.
- (7) (a) Stockigt, D. *J. Phys. Chem. A* **1997**, *101*, 3800. (b) Stockigt, D.; *Organometallics* **1999**, *18*, 1050.
- (8) Klippenstein, S. J.; Yang, C. N. *Int. J. Mass Spectrom.* **2000**, *201*, 253.
- (9) Kandalam, A. K.; Rao, B. K.; Jena, P.; Pandey R. *J. Chem. Phys.* **2004**, *120*, 10414.
- (10) Rao, B. K.; Jena, P. *J. Chem. Phys.* **2002**, *116*, 1343.
- (11) Shroder, D.; Loos, J.; Schwarz, H.; Thissen, R.; Preda, D. V.; Scott, L. T.; Caraiman, D.; Frach, M. V.; Bohme, D. K. *Helv. Chim. Acta* **2001**, *84*, 1625.
- (12) Frisch, M. J.; Trucks, G. W.; Schlegel, H. B.; Scuseria, G. E.; Robb, M. A.; Cheeseman, J. R.; Zakrzewski, V. G.; Montgomery, J. A.; Stratmann, R. E.; Burant, J. C.; Dapprich, S.; Millam, J. M.; Daniels, A. D.; Kudin, K. N.; Strain, M. C.; Farkas, O.; Tomasi, J.; Barone, V.; Cossi, M.; Cammi, R.; Mennucci, B.; Pomelli, C.; Adamo, C.; Clifford, S.; Ochterski, J.; Petersson, G. A.; Ayala, P. Y.; Cui, Q.; Morokuma, K.; Malick, D. K.; Rabuck, A. D.; Raghavachari, K.; Foresman, J. B.; Cioslowski, J.; Ortiz, J. V.; Stefanov, B. B.; Liu, G.; Liashenko, A.; Piskorz, P.; Komaromi, I.; Gomperts, R.; Martin, R. L.; Fox, D. J.; Keith, T.; Al-Laham, M. A.; Peng, C. Y.; Nanayakkara, A.; Gonzalez, C.; Challacombe, M.; Gill, P. M. W.; Johnson, B. G.; Chen, W.; Wong, M. W.; Andres, J. L.; Head-Gordon, M.; Replogle, E. S.; Pople, J. A. *Gaussian 98*; Gaussian Inc.: Pittsburgh, PA, 1998.
- (13) Hedberg, L.; Hedberg, K.; Cheng, P.; Scott, L. T. *J. Phys. Chem. A* **2000**, *104*, 7689.
- (14) Hanson, J. C.; Nordman, C. E. *Acta Crystallogr.* **1976**, *B32*, 1147.
- (15) Senapati, L.; Nayak, S. K.; Rao, B. K.; Jena, P. *J. Chem. Phys.* **2003**, *118*, 8671.
- (16) Pandey, R.; Rao, B. K.; Jena, P.; Blanco, M. A. *J. Am. Chem. Soc.* **2001**, *123*, 3799.
- (17) Scott, L.; Hashemi, M. M.; Bratcher, M. S. *J. Am. Chem. Soc.* **1992**, *114*, 1920.
- (18) Meyer, F.; Khan, I. A.; Armentrout, P. B. *J. Am. Chem. Soc.* **1995**, *117*, 9740.
- (19) Lewis, K. E.; Smith, G. P. *J. Am. Chem. Soc.* **1984**, *106*, 4650.